

Object Placement Planning and Optimization for Robot Manipulators

Joshua A. Haustein¹, Kaiyu Hang², Johannes Stork³ and Danica Kragic¹

Abstract—We address the problem of motion planning for a robotic manipulator with the task to place a grasped object in a cluttered environment. In this task, we need to locate a collision-free pose for the object that *a*) facilitates the stable placement of the object, *b*) is reachable by the robot manipulator and *c*) optimizes a user-given placement objective. Because of the placement objective, this problem is more challenging than classical motion planning where the target pose is defined from the start. To solve this task, we propose an anytime algorithm that integrates sampling-based motion planning for the robot manipulator with a novel hierarchical search for suitable placement poses. We evaluate our approach on a dual-arm robot for two different placement objectives, and observe its effectiveness even in challenging scenarios.

I. INTRODUCTION

Pick-and-place is among the most common tasks robot manipulators are applied for today. Grasp planning, which is the process of autonomously selecting grasps, still receives much attention and effort from the robotics community [1]–[3]. In contrast, the problem of placement planning, which is the process of autonomously deciding where and how to place an object with a robot, has received considerably less attention.

An autonomous robot tasked with placing a grasped object can generally not assume to know the environment in advance, rather it faces the following challenges when perceiving the environment for the first time:

1. It needs to identify suitable locations that afford placing. For instance, an object may be placed flat on a horizontal surface, leaned against a wall, placed on a hook, or laid on top of other objects. Determining how and where a particular object can be placed, requires analysis of both the environment’s and the object’s physical properties.
2. It needs to be able to reach the placement. Placing requires the robot to move close to obstacles, which make it difficult to compute collision-free arm configurations reaching a placement. In addition, the obstacles render planning an approach motion computationally expensive.
3. Not all placements are equally desirable. For many tasks, there exists an objective such as stability, human-preference on location or clearance from other obstacles, that is to be maximized.

¹ Division of Robotics, Perception and Learning (RPL), CAS, CSC, KTH Royal Institute of Technology, Stockholm, Sweden, E-mail: haustein, dani@kth.se

²GRAB Lab, Yale University, New Haven, USA, E-mail: kaiyu.hang@yale.edu

³Center for Applied Autonomous Sensor Systems (AASS), Örebro University, Örebro, Sweden, E-mail: johannesandreas.stork@oru.se

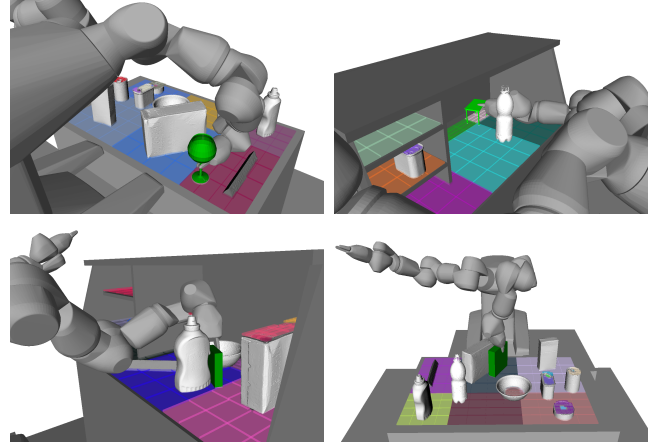


Fig. 1: Our algorithm computes placements for objects as well as corresponding approach motions in cluttered environments. In addition, it optimizes a user-specified objective for the placement pose. In the top row are example placements produced by our algorithm for a wine glass and toy table (*green*) under the objective to maximize clearance from other objects. In the bottom row a small and a large crayons box (*green*) are placed under the objective to minimize clearance.

Our contribution is an algorithmic framework that addresses these challenges and our main focus lies on computing reachable placement poses (challenge 2) that maximize a user-specified objective (challenge 3). In particular, we consider a dual-arm robot in difficult to navigate environments, such as cluttered shelves and cupboards, Fig. 1. Our approach addresses challenge 2 by integrating a motion planning algorithm with a novel hierarchical search for a placement pose. We address challenge 3 by designing the algorithm such that it finds an initial feasible solution quickly, and then incrementally improves the user-specified objective in an anytime fashion.

II. RELATED WORKS

A. Placing objects

Previous works on placing objects predominantly focus on challenge 1, i.e. searching poses in the environment, where an object can rest stably. A naïve solution consists in identifying horizontal surfaces in the environment and placing the object flat on the surface where there is enough space. This technique is, for instance, commonly employed in manipulation planning works which focus on planning complex sequences of pick-and-place operations rather than individual placements [4]–[8].

The object’s orientation for a horizontal placement can be obtained by analyzing the object’s convex hull and extracting the faces that support a stable placement [7], [8]. Each of

these faces gives rise to a base orientation when aligned with the support surface. Different poses with the same base orientation can then be obtained by translating the object on the support surface and rotating it around the surface’s normal. To locate collision-free and reachable placement poses (challenges 1 and 2), these works then employ rejection sampling of positions and orientations using a collision-checker and inverse kinematics solver. This is sufficiently efficient, if there are few obstacles and most sampled poses are within reach. If this is not the case, however, a more efficient strategy such as the one presented in this work is required.

More complex approaches to locating placement poses (challenge 1) have been presented by Schuster et al. [9], Harada et al. [10] and Jiang et al. [11]. Schuster et al. present a data-driven segmentation algorithm to discriminate clutter from support surfaces, and apply this segmentation to extract candidate placement poses. Similarly, Jiang et al. follow a data-driven approach and train a classifier to score the placement suitability of candidate poses based on manually defined features. These features are extracted from 3D point-clouds of the object and the environment, and include physical feasibility, stability, as well as human placement preference. The approach is capable of identifying a variety of placements, such as placing a plate in a dish-rack, hanging a mug on a bar or laying a box on a flat surface. In order to evaluate the classifier, however, the approach requires a set of candidate poses. Obtaining these in cluttered environments is non-trivial, as random sampling, for instance, has low probability of sampling good candidate.

Harada et al. [10] locate placement poses by matching planar surface patches on the object with planar surface patches in the environment. This allows the approach to locate placements on large, flat surfaces and also placements where the handle of a mug is hanging on a flat bar. While the work also integrates this algorithm with a motion planner (challenge 2), it does not perform any optimization of an objective (challenge 3).

In contrast to these previous works, our work’s focus lies on computing reachable placement poses among obstacles (challenge 2) that maximize a user-specified objective (challenge 3). We follow aforementioned previous works when addressing challenge 1 and place objects on horizontal support surfaces.

B. Integrated grasp and motion planning

Ensuring that a collision-free approach motion to a placement exists (challenge 2) requires us to closely integrate the placement search with a motion planning algorithm. This relates our problem to integrated grasp and motion planning [12]–[16]. These works present algorithms that simultaneously compute grasps with corresponding approach motions, and demonstrate that in cluttered environments separate planning of grasps and approach motions is inefficient. This is due to the fact that many potential grasps are in collision or out of reach. Our work addresses the analogous challenge for placing, with the extension of optimizing

an objective function on the placement (challenge 3). The method that we employ relates to our previous work on integrated grasp and motion planning [12].

III. PROBLEM DEFINITION

We consider a dual-arm robot equipped with two manipulators, $\mathcal{A} = \{1, 2\}$, that is tasked to place a *rigid* object o in a user-defined target volume $V \subset \mathbb{R}^3$ in its workspace. We assume that the object can be grasped by either arm, and the process of acquiring a stable grasp is known a priori. The target volume V is a set of positions for the object o and restricts the search space for placement poses to $\mathcal{X}^o = V \times SO(3) \subset SE(3)$. Obviously, not all poses in \mathcal{X}^o facilitate a stable placement, since for many of these the object might be, for example, in midair or intersecting obstacles. We denote the constraint that a pose $\mathbf{x} \in \mathcal{X}^o$ facilitates the stable placement of the object as binary mapping $s(\mathbf{x})$, that is 1 if \mathbf{x} is a stable placement and 0 otherwise. Additionally, we denote the constraint that a pose \mathbf{x} is physically feasible, i.e. that there is no intersection of the interior of the object with any obstacle, as binary predicate $c_f(\mathbf{x})$.

A placement pose must be reachable by the robot manipulator. For this, let $\mathcal{C}^a = \mathcal{C}_{\text{free}}^a \cup \mathcal{C}_{\text{obst}}^a$ denote the configuration space of arm $a \in \mathcal{A}$, and let $O(q): \mathcal{C}^a \rightarrow SE(3)$ denote the pose $\mathbf{x} \in SE(3)$ of the grasped object when the arm is in configuration $q \in \mathcal{C}^a$. We say a pose $\mathbf{x} \in \mathcal{X}^o$ is *path-reachable*, $r(\mathbf{x}) = 1$, if for some arm $a \in \mathcal{A}$ there exists a known collision-free continuous path $\tau: [0, 1] \rightarrow \mathcal{C}_{\text{free}}^a$ starting from the initial configuration of the robot $\tau(0) = q_0 \in \mathcal{C}_{\text{free}}^a$ and ending in a configuration $\tau(1) = q_g \in \mathcal{C}_{\text{free}}^a$ such that it reaches \mathbf{x} , i.e. $O(q) = \mathbf{x}$.

With these constraints and a user-provided objective function $\xi: \mathcal{X}^o \rightarrow \mathbb{R}$, we formalize our task as the following constraint optimization problem:

$$\begin{aligned} & \underset{\mathbf{x} \in \mathcal{X}^o}{\text{maximize}} && \xi(\mathbf{x}) \\ & \text{subject to} && c_f(\mathbf{x}) = 1 \\ & && s(\mathbf{x}) = 1 \\ & && r(\mathbf{x}) = 1 \end{aligned} \tag{1}$$

Independently of the objective function, the optimization problem is challenging to solve due to the constraints. The collision-free constraint $c_f(\mathbf{x})$ renders the problem non-convex. The stability constraint, $s(\mathbf{x})$, is difficult to model, as it is a function of the physical properties of the object and the local environment. Lastly, the path-reachability constraint $r(\mathbf{x})$ requires a motion planning algorithm to compute an approach path, which is generally computationally expensive.

Note that after releasing an object at a placement pose, the robot might not be able to retreat without colliding with the placed object. Hence, in principle, there is the additional constraint that a collision-free retreat motion must be possible. In this work, however, we choose to exclude this constraint from our problem definition and instead assume that a collision-free retreat is always possible.

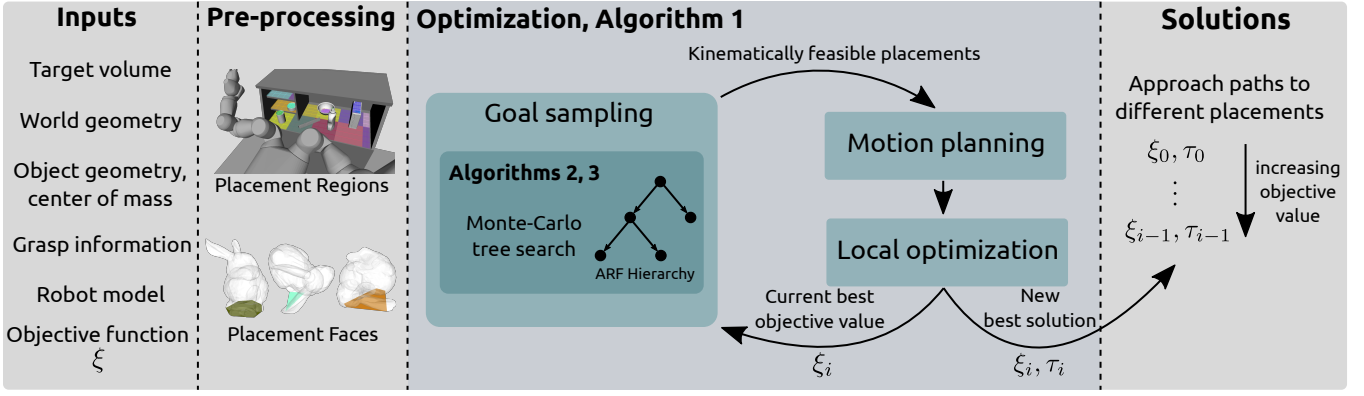


Fig. 2: Our approach consists of two stages. In a pre-processing stage we first extract placement regions and faces that help locating us stable object poses. In the optimization stage a sampling algorithm is employed to locate kinematically reachable and collision-free stable placement poses. These are provided to a motion algorithm to verify path-reachability and construct an approach motion. Subsequently a local optimization algorithm is employed to improve the placement locally. Any found solution is made available to the user, and subsequent iterations search for better solutions.

A. Assumptions on prior information

We assume access to the kinematic and geometric model of the robot, the geometry of the object, the location of its center of mass, and the geometry of the environment in form of surface points $S \subset \mathbb{R}^3$. Furthermore, we assume that the environment is rigid, and that gravity acts antiparallel to the z -axis of the world’s reference frame.

We also assume that for each manipulator $a \in \mathcal{A}$ the grasp transformation matrices ${}^gT_o^a \in SE(3)$ from the object’s frame to the respective gripper frame are known. We assume that these grasps are selected such that a stable placement pose can be acquired without releasing the object.

For a pose $\mathbf{x} \in SE(3)$, let $\mathbf{p}_x = (x, y, z) \in \mathbb{R}^3$ be its position and $\mathbf{o}_x = (e_x, e_y, e_z)$ its orientation expressed in rotation angles around the world’s x, y and z axis respectively. Our algorithm treats the objective function $\xi(\mathbf{x})$ as a black-box, however, we will assume that the function is numerically differentiable w.r.t. the x, y, e_z components of \mathbf{x} .

IV. METHOD

We address the problem in Eq. (1) with the framework shown in Fig. 2. This framework consists of a pre-processing stage and an optimization stage, Algorithm 1. The framework receives the information listed on the left as input and produces paths $\tau_i : [0, 1] \rightarrow \mathcal{C}_{\text{free}}^a$ for the different arms $a \in \mathcal{A}$ as output. The final configuration of each path $\tau_i(1)$ represents a placement solution using a particular arm, and places the object at a stable and collision-free placement pose $\mathbf{x} = O(\tau_i(1))$. The optimization algorithm, Algorithm 1, operates in an anytime fashion, meaning that it iteratively produces new solutions $\tau_{i'}$ that achieve better objective $\xi_{i'}^l = \xi(O(\tau_{i'}(1)))$ than the previous solutions $\tau_i, i < i'$.

The base idea of our approach is to decompose the problem into a search for feasible placement poses that fulfill all constraints, and only subsequently optimize the objective. In general, we can not model all of the constraints in Eq. (1) in closed form. However, for a particular pose $\mathbf{x} \in \mathcal{X}^o$ we can verify whether it fulfills the constraints. We

therefore address the optimization problem in a sampling-based manner. For each constraint in Eq. (1) our framework has a component designed to verify it or to provide samples fulfilling it:

Stable placement. A necessary condition for a pose $\mathbf{x} \in \mathcal{X}^o$ to be stable, $s(\mathbf{x}) = 1$, is that the object is in contact with the environment. Therefore, in the pre-processing stage, we extract surfaces in the target volume and on the object that afford placing. With these surfaces we can obtain an approximation $\hat{S} \subset \mathcal{X}^o$ of the set of stable placement poses that serves as search space for our optimization. In addition, these surfaces allow us to verify, whether the object is placed stably at a given pose.

Physically feasible placement. Within the set \hat{S} we need to locate object poses that are physically feasible, $c_f(\mathbf{x}) = 1$, i.e. poses that do not result in penetration of any obstacles. In addition, we need to verify that these poses can be reached by collision-free arm configurations $q \in \mathcal{C}_{\text{free}}^a$ for at least one arm, as this is a necessary condition for a placement pose to be path-reachable, $r(\mathbf{x}) = 1$. This verification as well as the sampling is performed within Algorithm 2, which we refer to as goal sampling algorithm.

Reachable placement. To verify the path-reachability of candidate poses, $r(\mathbf{x}) = 1$, we need to construct approach paths to them. For this, we employ a sampling-based motion planning algorithm [17] that receives arm configurations sampled by the goal sampling algorithm as goals.

Preferred placement. The optimization of the objective function is achieved through two concepts. First, we employ a greedy local optimization algorithm on the poses for which all constraints have been verified to be fulfilled. Second, whenever the motion planner succeeds in verifying path reachability for a new pose sample \mathbf{x} , we constrain following iterations to only validate path-reachability for poses \mathbf{x}' that achieve a better objective $\xi(\mathbf{x}') > \xi(\mathbf{x})$.

A. Defining Potential Contacts

Modeling the set of stable poses $S = \{\mathbf{x} \in \mathcal{X}^o \mid s(\mathbf{x}) = 1\}$ of stable placement poses is challenging, due to the large variety of possible placements. While we only require

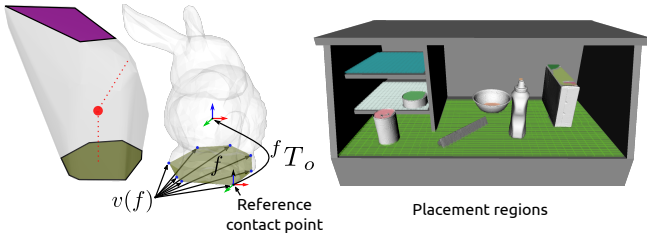


Fig. 3: Placement faces and regions. *Left:* The Stanford bunny model is shown with its convex hull and two of the hull’s faces are highlighted (purple and green). By projecting the center of mass (red) along the faces’ normals, we can determine which face supports a stable horizontal placement. For faces $f \in \mathcal{F}$ that support a placement, we refer by $v(f)$ to its vertices and by ${}^f T_o$ to the transformation matrix from a reference vertex to the object’s frame. *Right:* We extract contiguous horizontal surfaces in the environment that provide us with candidate location to place the object at.

samples from this set, rejection sampling on \mathcal{X}^o does not suffice, due to low probability of satisfying the constraint $s(x) = 1$. We therefore approximate this set by the set of poses at which the object is placed on horizontal surfaces. For this, we extract a discrete set of *placement contact regions*, $\mathcal{R} = \{r_i\}_{i=1}^m, r_i \subset \mathcal{S} \cap V \subsetneq \mathbb{R}^3$, from the surface geometry in the target volume. A placement contact region is a contiguous set of surface points that share the same height, see Fig. 3. In our implementation, we extract these from an occupancy grid of the environment, however, also other techniques could be employed.

To determine the orientation in which the object should make contact with these regions, we extract contact points from the object’s surface. For this, we follow a similar approach as in aforementioned previous works [7], [8] and select faces from the object’s convex hull to place the object on. The convex hull of a finite set of points, i.e. a point cloud of the object, is a convex polyhedron. A face of this polyhedron supports a stable placement on a horizontal surface, if the projection of the object’s center of mass along the face’s normal falls into this face, see Fig. 3. We refer to the $k \in \mathbb{N}$ number of faces for which this is the case as *placement faces*, $\mathcal{F} = \{f_i\}_{i=1}^k$.

Only the vertices of the boundary of a placement face, $v(f)$, are guaranteed to be part of the actual object’s surface. It is therefore these vertices that need to be in contact with the support surface in order for the object to be placed stably. For each face, we select one of these vertices as reference contact point and define a transformation matrix ${}^f T_o$ as shown in Fig. 3. With this, the combination of a contact region $r \in \mathcal{R}$ and a placement face $f \in \mathcal{F}$ defines a class of object poses

$$\hat{S}(r, f) = \left\{ T(R_z(\theta), \begin{pmatrix} x \\ y \\ z_r \end{pmatrix}) {}^f T_o \mid \begin{pmatrix} x \\ y \\ z_r \end{pmatrix} \in r, \theta \in [0, 2\pi) \right\},$$

where z_r is the z -coordinate of the placement region, $R_z(\theta)$ the rotation matrix around the z -axis by angle θ , and $T(\cdot, \cdot)$ an operator that combines these to a transformation matrix. These poses vary in x, y translation within the contact region and rotation by θ around the z -axis going through the reference point located at x, y, z_r . The union $\hat{S} =$

Algorithm 1: High-level Placement Planner

```

1  $M_s, G_s \leftarrow \emptyset, \emptyset$  // Storage of internal state
2  $\tau, \xi_{\text{best}}, \mathcal{G} \leftarrow \perp, -\infty, \emptyset$ 
3 while not TERMINATE()
4    $G_n, G_s \leftarrow \text{SAMPLEGOALS}(g_{\text{max}}, \xi_{\text{best}}, G_s)$ 
5    $\mathcal{G} \leftarrow \mathcal{G} \cup G_n$ 
6   if  $|\mathcal{G}| > 0$ 
7      $\tau, M_s \leftarrow \text{PLANMOTION}(m_{\text{max}}, \mathcal{G}, M_s)$ 
8     if  $\tau \neq \perp$ 
9        $\tau \leftarrow \text{OPTIMIZELOCALLY}(\tau)$ 
10       $\tau_{\text{best}} \leftarrow \tau$ 
11       $\xi_{\text{best}} \leftarrow \xi(O(\tau(1)))$ 
12       $G_o = \{g \in \mathcal{G} \mid \xi(O(g)) \leq \xi_{\text{best}}\}$ 
13       $\mathcal{G} = \mathcal{G} \setminus G_o$ 
14      publish  $\tau_{\text{best}}, O(\tau_{\text{best}}(1))$ 
15 return  $\tau_{\text{best}}, O(\tau_{\text{best}}(1))$ 

```

$\bigcup_{r \in \mathcal{R}, f \in \mathcal{F}} \hat{S}(r, f)$ of all these sets is then a parameterized approximation of S that we can search for feasible placements.

Note that not all poses in \hat{S} are stable, since it’s definition only guarantees that the reference contact point is in contact with the placement contact region. To verify that a pose $x \in \hat{S}$ is actually stable, we need to verify that all vertices of the respective placement face are in contact with a placement region. They may, however, be in contact with different regions, which allows placements where, for instance, an object is placed over a gap in the support surface.

B. Sampling-based Optimization

The optimization of the objective is performed by Algorithm 1. The algorithm alternates between executing the sub-algorithms SAMPLEGOALS, PLANMOTION and OPTIMIZELOCALLY until termination is requested by the user. SAMPLEGOALS computes a finite set of collision-free arm configurations $G_n = \{(q, a) \mid a \in \mathcal{A}, q \in \mathcal{C}_{\text{free}}^a\}$, such that for each $q \in G_n$ the stability constraint, $s(O(q)) = 1$, and the physical feasibility constraint, $c_f(O(q)) = 1$, are fulfilled. Furthermore, it only returns configurations for which the placement objective improves over the best solution found so far, $\xi(O(q)) > \xi_{\text{best}}$. Initially, ξ_{best} is set to $-\infty$ and is updated, whenever the motion planner succeeds at finding a new path τ to any of the configuration $q \in \mathcal{G}$, where \mathcal{G} stems from the union of all sampled goals.

Motion planning towards the goals, \mathcal{G} , is performed in PLANMOTION. The set \mathcal{G} is maintained to only contain configurations that reach placements of greater objective than ξ_{best} . This guarantees that whenever a new path is found, it reaches a placement with a better objective than any previous solution. Subsequent to finding a new path, OPTIMIZELOCALLY is executed to further improve the solution locally.

In each iteration SAMPLEFEASIBLE and PLANMOTION receive parameters $g_{\text{max}}, G_s, m_{\text{max}}, M_s$ respectively. The presence of the parameters G_s, M_s emphasizes that both sub-algorithms maintain an internal state across iterations of the algorithm, which is crucial for the efficiency of the overall approach and will be detailed in the following sections. The parameters $g_{\text{max}}, m_{\text{max}}$ limit the computation time budget for each function, to balance the computational burden of sampling new goals and planning motions to sampled ones.

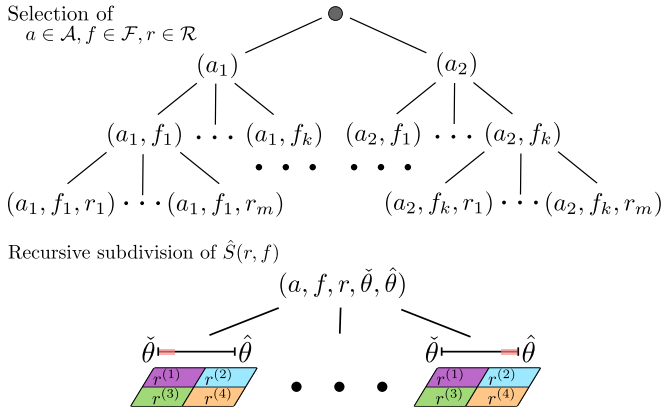


Fig. 4: The AFR hierarchy constitutes of two different parts. On the first three level, the hierarchy represents choices of an arm $a \in \mathcal{A}$, a placement face $f \in \mathcal{F}$ and a region $r \in \mathcal{R}$. On the level at greater depths, the hierarchy recursively subdivides the region r and the range of orientations $[\hat{\theta}, \check{\theta}]$ within a pose set $\hat{S}(r, f)$

C. Sampling Kinematically Feasible Placements

The function `SAMPLEGOALS` needs to solve a constraint satisfaction problem:

$$\begin{aligned}
 &\text{find} && a \in \mathcal{A}, q \in \mathcal{C}^a \\
 &\text{such that} && \xi(O(q)) > \xi_{\text{best}} \\
 &&& s(O(q)) = 1 \\
 &&& c_f(O(q)) = 1 \\
 &&& q \in \mathcal{C}_{\text{free}}^a.
 \end{aligned} \tag{2}$$

This subproblem by itself is challenging to solve. While we only require samples from the feasible set of this problem, rejection sampling on \mathcal{C}^a , $a \in \mathcal{A}$ does not suffice, due to low or zero probability of satisfying $s(O(q)) = 1$. Hence, instead we sample the parameterized pose set \hat{S} , for which it likely that $s(x)$ is fulfilled, and employ an inverse kinematics solver to compute arm configurations for the sampled poses. This, however, can be rather inefficient in the presence of obstacles, where the probability of randomly sampling a collision-free object pose x and arm configuration $q \in \mathcal{C}^a$ reaching x is low. We remedy this by employing a sampling procedure that adapts its sampling and focuses on regions of \hat{S} that are likely to fulfill all constraints.

1) *AFR-Hierarchy*: Sampling a pose from \hat{S} involves choosing a placement contact region $r \in \mathcal{R}$ and a placement face $f \in \mathcal{F}$. In addition, to compute an arm configuration reaching a sampled pose, we need to select an arm $a \in \mathcal{A}$. While there is an overlap of the poses that each arm can reach, some may be more easily reached by one than the other. Whether a particular placement face f is a good choice to place an object on depends on the grasp, and thus on the arm that is selected. Similarly, whether a placement region allows a stable and obstacle penetration free placement strongly depends on the placement face, as this determines the footprint and the base orientation of the object. Furthermore, if a pose $x \in \hat{S}(r, f)$ for a particular region r and face f is reachable by an arm a , it is likely that poses in close proximity are also reachable by the arm. Hence, there exists a spatial correlation of feasibility within

a set $\hat{S}(r, f)$, as well as between different sets of $\hat{S}(r, f)$ with similar categorical choices for $r \in \mathcal{R}$, $f \in \mathcal{F}$ and arms $a \in \mathcal{A}$.

This observation leads us to the definition of the AFR-hierarchy shown in Fig. 4. On the first level of this hierarchy, an arm $a \in \mathcal{A}$ is selected, on the second level a placement face $f \in \mathcal{F}$, and on the third a placement contact region $r \in \mathcal{R}$. From the third level on, each node in the hierarchy defines all quantities that we require to sample poses and compute arm configurations. Subsequent level of this hierarchy recursively partition the sets $\hat{S}(r, f)$. On these lower level, every node represents a tuple $(a, r, f, \check{\theta}, \hat{\theta})$, where $\check{\theta}, \hat{\theta}$ define a range of orientation angles. The nodes at depth 3 cover all of $\hat{S}(r, f)$ and thus it is $\check{\theta} = 0$ and $\hat{\theta} = 2\pi$. The children of this node, however, will only cover subsets of $\hat{S}(r, f)$ that are constrained in the positions and orientations.

Let $n^{(i)} = (a, r^{(i)}, f, \check{\theta}^{(i)}, \hat{\theta}^{(i)})$ be a node at depth $i \geq 3$, then the children of this node arise from subdividing the region $r^{(i)}$ and the interval $[\check{\theta}^{(i)}, \hat{\theta}^{(i)}]$. The placement region $r^{(i)}$ is divided into four subregions $r^{(i)} = r_1^{(i)} \cup r_2^{(i)} \cup r_3^{(i)} \cup r_4^{(i)}$ by splitting it along its mean x and y positions. The interval $[\check{\theta}^{(i)}, \hat{\theta}^{(i)}]$ is split into l equally sized sub-intervals. The resulting $l \times 4$ children of $n^{(i)}$ then arise from combining each subregion with each interval of the orientation ranges. This subdivision is continued until some user-specified minimal region area and interval length.

2) *Monte Carlo Tree Search-based Goal Sampling*: To obtain samples that satisfy Eq. (2) we exploit the aforementioned correlation and employ a Monte Carlo Tree search (MCTS) [18]-based algorithm for sampling. The algorithm is shown in Algorithm 2 and Algorithm 3, and uses the AFR-hierarchy to produce the desired samples. Algorithm 2 is the `SAMPLEGOAL` procedure that is called by Algorithm 1.

The key idea of the algorithm is that it incrementally constructs a tree of the nodes in the AFR hierarchy, and stores for each node the proportion of valid samples that have been obtained from its subbranch. This knowledge is then used to focus sampling on branches of the hierarchy that are likely to contain valid samples, while still maintaining some exploration. The tree is stored in the variable G_s , and thus steadily constructed across all executions of `SAMPLEGOAL` in Algorithm 1.

Every time Algorithm 2 is executed it attempts to produce g_{max} goal samples (q, a) , where $q \in \mathcal{C}_{\text{free}}^a$ is a collision-free arm configuration for arm a reaching a feasible placement pose, $s(O(q)) = 1$, $c_f(O(q)) = 1$ that improves the objective $\xi(O(q)) > \xi_{\text{best}}$. For each sample, the algorithm first selects a node n from the AFR hierarchy using Algorithm 3. Algorithm 3 ensures that this node fully specifies a set $\hat{S}(r, f)$ or a subset thereof as described in IV-C.1. It then randomly samples a pose from this set and evaluates whether the pose constraints $c_f(x), s(x)$ and $\xi(x) > \xi_{\text{best}}$ are fulfilled. If this is the case, it employs an inverse kinematics solver to compute an arm configuration $q \in \mathcal{C}^{a_n}$ for the arm a_n specified by the AFR node n . If such a configuration exists and it is collision-free, we obtained a new goal sample that can be provided to the motion planning algorithm.

Algorithm 2: SAMPLEGOALS: Monte-Carlo Tree search based sampling algorithm

Input: Number of maximal iterations g_{\max} , best achieved objective value ξ_{best} , state storage G_s
Output: Feasible placement configurations \mathcal{G}_n , state storage G_s

```

1  $\mathcal{G}_n \leftarrow \emptyset$ 
2 for  $i \leftarrow 1, \dots, g_{\max}$ 
3    $n \leftarrow \text{SELECTAFRNODE}(G_s)$ 
4    $\mathbf{x} \leftarrow \text{SAMPLE}(n)$ 
5   if  $s(\mathbf{x}) = 1 \wedge c_f(\mathbf{x}) = 1 \wedge \xi(\mathbf{x}) > \xi_{\text{best}}$ 
6      $q \leftarrow \text{IKSOLVER}(\mathbf{x}, a_n)$ 
7     if  $q \in \mathcal{C}_{\text{free}}^{a_n}$ 
8        $\mathcal{G}_n \leftarrow \mathcal{G}_n \cup \{(q, a_n)\}$ 
9    $\text{UPDATE}(n, G_s, \mathbf{x}, q, \xi_{\text{best}})$ 
10 return  $\mathcal{G}_n, G_s$ 

```

After each sample step, the tree stored in G_s is updated according to whether we successfully obtained a new goal sample or not. For each sampled node n , we store the following information in G_s :

- $v(n)$, the number of samples obtained from n or any of its descendants
- $r(n)$, the sum of all rewards obtained for sampling n or any of its descendants
- $Ch(n, G_s)$, the children of n that have been added to G_s

The numbers $v(n)$ and $r(n)$ are updated by the UPDATE function, whereas $Ch(n, G_s)$ is updated within Algorithm 3. When we sampled n we obtain a reward

$$\Delta r(n) = \begin{cases} H(\mathbf{x}, q, \xi_{\text{best}}) & \text{if } n \text{ is not a leaf of AFR} \\ 1 & \text{if } v(\mathbf{x}, q, \xi_{\text{best}}) = 1 \\ 0 & \text{otherwise} \end{cases} \quad (3)$$

where $v(\mathbf{x}, q, \xi_{\text{best}}) = 1$, if all constraints are fulfilled, i.e. $s(\mathbf{x}) = 1, c_f(\mathbf{x}) = 1, \xi(\mathbf{x}) > \xi_{\text{best}}$ and $q \in \mathcal{C}_{\text{free}}^a$. This reward is binary, if n is a leaf of the AFR hierarchy and there are no further subdivisions of the pose set. If n , however, is not a leaf, the reward is a heuristic value $H(\mathbf{x}, q, \xi_{\text{best}}) \in [0, 1]$ that also gives non-zero rewards to samples that fulfill some, but not all of the constraints. In any case, the reward is recursively propagated to the ancestors n' of n to update their respective $v(n'), r(n')$. The number of samples, $v(n')$, is always increased by one as we acquired a single sample, whereas the accumulated reward $r(n')$ is updated by the reward $\Delta r(n)$ obtained by the sampled node n .

The decision on which node to sample is made in the SELECTAFRNODE function, Algorithm 3. The algorithm always starts at the root of the AFR hierarchy and descends to a node in the hierarchy that it decides to sample. Since we can produce samples only for nodes at depths greater than 3, the algorithm always needs to descend at least to depth 3 before returning any node. For nodes n at depth greater than 3 the algorithm descends to its children, as long as n is not a leaf and n has been sampled before.

Initially, G_s only contains the root of the AFR hierarchy. Hence, the only option the algorithm has is to select a child in the AFR hierarchy that is not in G_s yet. This is done by the ADDCHILD operation, which selects a random child

Algorithm 3: SELECTAFRNODE: Selection of node AFR-hierarchy

Input: State storage G_s
Output: node n in G_s that defines a tuple $(a, f, r, \tilde{\theta}, \hat{\theta})$

```

1 Function SELECTCHILD( $n, G_s$ )
2   for  $i \in Ch(n, G_s)$ 
3      $u_i \leftarrow \frac{r(i)}{v(i)} + c\sqrt{\frac{2\ln(v(n))}{v(i)}}$ 
4    $u' \leftarrow -\infty$ 
5   if  $|Ch(n, G_s)| < |Ch(n)|$ 
6      $u' \leftarrow \frac{1}{j} \sum_{i=1}^j \frac{r(i)}{v(i)} + c\sqrt{\frac{2\ln(v(n))}{j}}$ 
7   if  $\forall i \in Ch(n, G_s) : u' > u_i \vee |Ch(n, G_s)| = 0$ 
8     return ADDCHILD( $n, G_s$ )
9   return  $\arg \max_{i \in Ch(n, G_s)} u_i$ 
10  $n \leftarrow \text{ROOT}(G_s)$ 
11 for  $d \leftarrow 1 \dots 3$ 
12    $n \leftarrow \text{SELECTCHILD}(n, G_s)$ 
13 while  $v(n) > 0 \wedge \neg \text{ISLEAF}(n)$ 
14    $n \leftarrow \text{SELECTCHILD}(n, G_s)$ 
15 return  $n$ 

```

from the AFR hierarchy and adds it to G_s . Let n now be any selected AFR node that is already stored in G_s . We distinguish between its children $Ch(n, G_s)$ that are also stored in G_s and its total set of children $Ch(n)$ as defined by the hierarchy. If n has children in G_s , the algorithm may either descend to one of them, or add a new child to G_s , if $|Ch(n, G_s)| < |Ch(n)|$. The decision on what to do is based on the UCB1 policy [19], which is common to employ in Monte-Carlo Tree search and shown in Algorithm 3. It allows to the algorithm to balance between re-sampling branches (exploitation) that have led to valid samples before and exploring new branches. The score u' for adding a new child is based on the conservative assumption that any unsampled node is as good as the average of its siblings.

D. Motion Planning

The subalgorithm PLANMOTION plans motions for each arm separately, as we assume that only one arm is required to perform the actual placement, while all other arms remain in a resting position. In principle, any motion planning algorithm could be employed for this subalgorithm. The only requirement on the algorithm is the possibility to efficiently add and remove goal configurations from the goal set \mathcal{G} , desirably without losing information, e.g. samples in a search tree, that could be beneficial for planning paths to future goals.

In our implementation, we employ a modification of OMPL's [20] bidirectional RRT algorithm [21]. The algorithm constructs a single forward tree and one backward tree for each goal in \mathcal{G} . Whenever the algorithm succeeds in connecting the forward tree with a backward tree, the two trees are merged and success is reported. When \mathcal{G} is modified, the backward trees rooting in goal configurations that have been removed are still maintained, as they may still prove valuable to reach other goals. When connecting to any of these, however, the algorithm no longer reports success and only merges it into the forward tree.

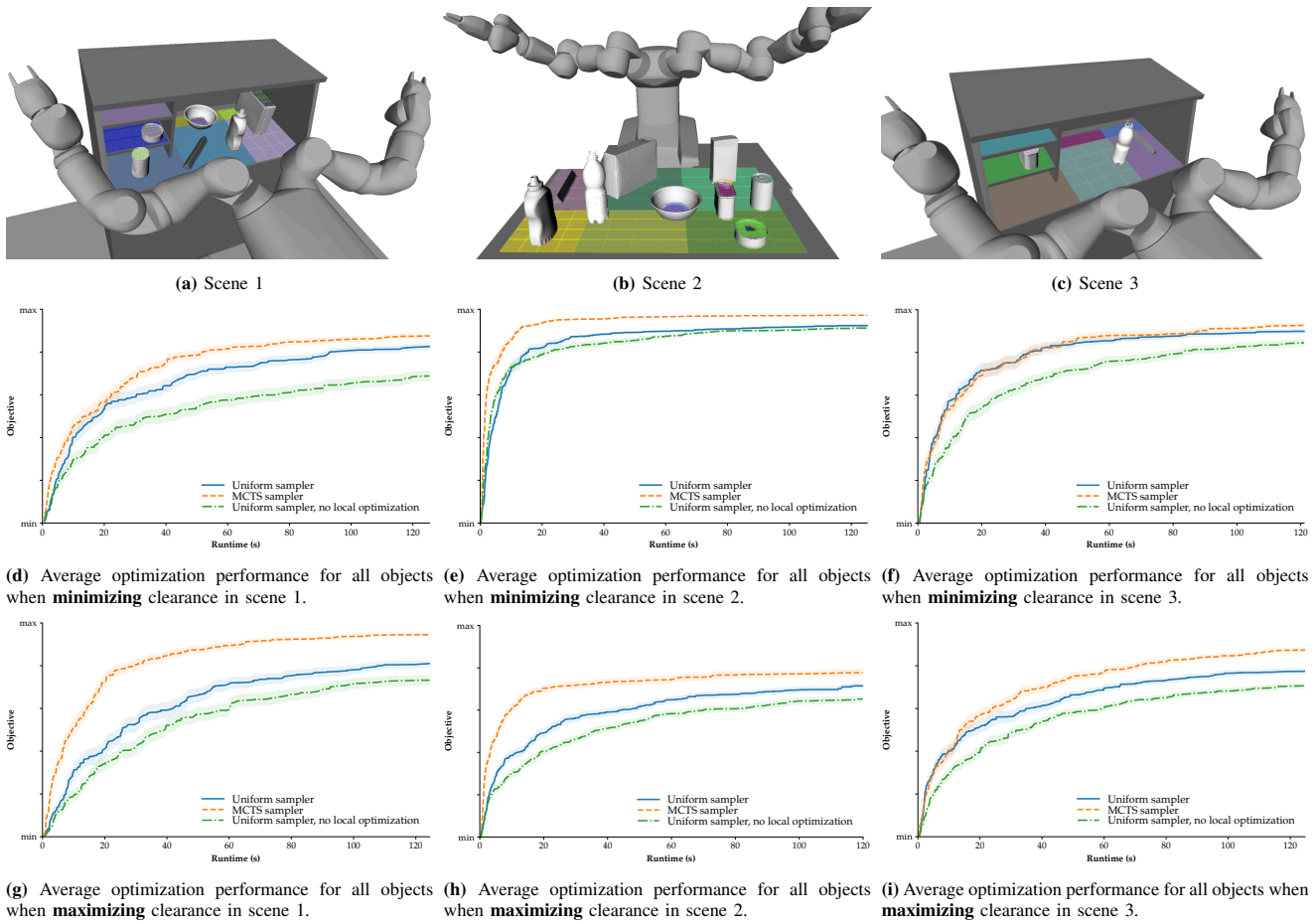


Fig. 5: Experiments scenes and optimization performance of different instances of our algorithm. The plots in (d) - (i) show the mean relative objective achieved by each algorithm as a function of planning time. The plots show the average optimization performance across all test objects. In order to make the objective values comparable, we normalize the achieved objective values for each scene and object into the range of minimal and maximal objective observed throughout all executions.

E. Local Optimization

Whenever the motion planning algorithm succeeds in computing a new path τ_i , we locally optimize the reached placement pose by following the gradient of the objective function ξ . For this, let $q = \tau_i(1)$ be the final configuration of the path that reaches a placement pose $O(q) = \mathbf{x}$. We can locally improve the solution using the following update rule:

$$\Delta q \leftarrow J^\dagger v\left(\frac{\partial \xi}{\partial x, y, e_z}(O(q))\right)$$

$$q \leftarrow q + \mu \Delta q,$$

where J^\dagger is the pseudo-inverse of the arm's Jacobian at q , $\mu \in \mathbb{R}^{>0}$ a step size, and $v(x, y, \theta) = (x, y, 0, 0, 0, \theta)^T$ lifts the three dimensional gradient to a six dimensional end-effector velocity. As long as the updated q is collision-free and $O(q)$ is not violating any constraints, we concatenate the new configurations to the path τ and obtain an improved feasible solution.

V. EXPERIMENTS

We implemented our approach in Python using OpenRAVE [22] and the Open Motion Planning Library [20]. For evaluation, we plan and optimize placements for four

different objects on three different environments with varying degree of clutter, see Fig. 1 and Fig. 5. The objects differ in size, shape and in number of placement faces. As robot model, we employ ABB's dual-arm robot Yumi, where each arm has 7 DoFs. All experiments were run on an Intel Core i7-4790K CPU @ 4.00GHz×4 with 16GB RAM running Ubuntu 18.04.

As objective function we employ two variations of clearance to obstacles within the placement volume. We define the clearance to obstacles as:

$$C(\mathbf{x}) = \frac{1}{|\mathcal{B}_o(\mathbf{x})|} \sum_{\mathbf{p}' \in \mathcal{B}_o(\mathbf{x})} d_S(\mathbf{p}'), \quad (4)$$

where $\mathcal{B}_o(\mathbf{x})$ denotes a finite set of points approximating the volume of o when it is located at pose \mathbf{x} . The function $d_S : \mathbb{R}^3 \rightarrow \mathbb{R}$ denotes the distance in x, y and positive z direction to the environment's surface within the target volume V . Maximizing this function, i.e. $\xi(\mathbf{x}) = C(\mathbf{x})$, leads to placements where the object is distant to obstacles. This is useful, for example, if the robot is tasked with manipulating the object further after placing. Minimizing this clearance function, i.e. $\xi(\mathbf{x}) = -C(\mathbf{x})$, on the other hand, is a good heuristic when the robot is tasked to pack

multiple objects into a limited volume. This objective is particularly interesting, as the closer the object is to be placed to obstacles, the more difficult it is to obtain a collision-free approach path.

As can be seen in Fig. 1, and better so in the accompanying video, our algorithm succeeds at computing placements with high objective values for all test cases. To evaluate the planning and optimization performance of our approach, we compare it to two simplified modifications. In the first modification, we replace the Monte-Carlo Tree search-based sampling algorithm, Algorithm 2, with a naive uniform sampler. In addition, in the second modification we remove the local optimization from Algorithm 1.

We ran each instance for each objective, object and scene 20 times for 2 minutes and recorded the objective values of the found solutions. The progress of the average objective values as a function of runtime is shown in Fig. 5.

In all test cases all instances of our algorithm compute initial solutions within a few seconds, and succeed at locating better solutions as time progresses. We observe that our algorithm using MCTS performs better than, or as good, as the baselines. The uniform sampler without local optimization performs worse than the one with. Hence, we conclude it is both the local optimization and the MCTS sampling that enable our algorithm to find better solutions faster, and on average achieve larger final objectives.

The mean objective values increase quickly in the beginning before slowing down as they approach the maximum objective ever observed in the respective scene. This is likely due to the fact that the probability of locating poses that improve the objective declines the higher the best achieved objective is.

VI. DISCUSSION & CONCLUSION

We presented an algorithmic framework that computes robot motions to transport a grasped object to a stable placement that optimizes a user-provided objective. Our approach is capable of achieving this even in environments cluttered with obstacles. The approach considers all available arms to reach the best placement and operates in an anytime-fashion, computing initial low-objective solutions quickly and improving on it as computational resources allow.

Our approach combines sampling-based motion planning and local optimization with a hierarchical sampling algorithm based on MCTS. A key novelty lies in the AFR hierarchy and applying MCTS as sampling algorithm. While our experiments already demonstrate the advantage of this approach, we believe it has more potential. For instance, in this work the grasp, that we place the object with, is determined by the chosen arm. An interesting future extension is to incorporate different choices of grasps into the hierarchy. In addition, the sampling algorithm could employ pruning of branches of the hierarchy, if a branch can be proven to not contain any solutions.

Further, we believe the approach can be extended to different types of placements. The different combinations of placement faces and regions constitute disjoint contact

classes of object poses. In future work, we intend to extend the AFR hierarchy to more diverse contact classes, such as an object leaning against a wall.

Lastly, one of the weaknesses of the sampling-based optimization approach is the decreasing convergence rate observed in our experiments. To remedy this, we intend to investigate whether we can exploit gradient information not only in the local optimization step, but also in the goal sampling algorithm.

REFERENCES

- [1] A. Bicchi and V. Kumar, "Robotic grasping and contact: A review," in *ICRA*, 2000.
- [2] J. Bohg, A. Morales, T. Asfour, and D. Kragic, "Data-driven grasp synthesis – a survey," *TRO*, vol. 30, no. 2, 2014.
- [3] M. Roa and R. Suárez, "Grasp quality measures: review and performance," *Auton. Robots*, vol. 38, no. 1, 2015.
- [4] P. S. Schmitt, W. Neubauer, W. Feiten, K. M. Wurm, G. V. Wichert, and W. Burgard, "Optimal, sampling-based manipulation planning," in *ICRA*, May 2017.
- [5] Z. Xian, P. Lertkultanon, and Q. Pham, "Closed-chain manipulation of large objects by multi-arm robotic systems," *IEEE RA-L*, vol. 2, no. 4, pp. 1832–1839, Oct 2017.
- [6] C. R. Garrett, T. Lozano-Pérez, and L. P. Kaelbling, "FFRob: Leveraging symbolic planning for efficient task and motion planning," *IJRR*, vol. 37, no. 1, pp. 104–136, 2018.
- [7] W. Wan, H. Igawa, K. Harada, H. Onda, K. Nagata, and N. Yamanobe, "A regrasp planning component for object reorientation," *Autonomous Robots*, pp. 1–15, jul 2018.
- [8] P. Lertkultanon and Q. Pham, "A certified-complete bimanual manipulation planner," *IEEE Transactions on Automation Science and Engineering*, vol. 15, no. 3, pp. 1355–1368, July 2018.
- [9] M. J. Schuster, J. Okerman, H. Nguyen, J. M. Rehg, and C. C. Kemp, "Perceiving clutter and surfaces for object placement in indoor environments," in *Humanoids*, Dec 2010, pp. 152–159.
- [10] K. Harada, T. Tsuji, K. Nagata, N. Yamanobe, and H. Onda, "Validating an object placement planner for robotic pick-and-place tasks," *Robotics and Autonomous Systems*, vol. 62, no. 10, pp. 1463 – 1477, 2014.
- [11] Y. Jiang, M. Lim, C. Zheng, and A. Saxena, "Learning to place new objects in a scene," *IJRR*, vol. 31, no. 9, pp. 1021–1043, 2012.
- [12] J. A. Hausteijn, K. Hang, and D. Kragic, "Integrating motion and hierarchical fingertip grasp planning," in *ICRA*, May 2017, pp. 3439–3446.
- [13] J. Rosell, R. Suárez, and A. Pérez, "Path planning for grasping operations using an adaptive pca-based sampling method," *Auton. Robots*, 2013.
- [14] D. Berenson, R. Diankov, K. Nishiwaki, S. Kagami, and J. Kuffner, "Grasp planning in complex scenes," in *Humanoids*, 2007.
- [15] N. Vahrenkamp, T. Asfour, and R. Dillmann, "Simultaneous grasp and motion planning: Humanoid robot armar-iii," *IEEE Robotics Automation Magazine*, 2012.
- [16] J. Fontanals, B. A. Dang-Vu, O. Porges, J. Rosell, and M. A. Roa, "Integrated grasp and motion planning using independent contact regions," in *Humanoids*, Nov 2014.
- [17] M. Elbanhawi and M. Simic, "Sampling-based robot motion planning: A review," *IEEE Access*, vol. 2, pp. 56–77, 2014.
- [18] C. B. Browne, E. Powley, D. Whitehouse, S. M. Lucas, P. I. Cowling, P. Rohlfshagen, S. Tavener, D. Perez, S. Samothrakis, and S. Colton, "A survey of monte carlo tree search methods," *IEEE Transactions on Computational Intelligence and AI in Games*, vol. 4, no. 1, pp. 1–43, March 2012.
- [19] P. Auer, N. Cesa-Bianchi, and P. Fischer, "Finite-time analysis of the multiarmed bandit problem," *Machine Learning*, vol. 47, no. 2, pp. 235–256, May 2002.
- [20] I. A. Şucan, M. Moll, and L. E. Kavraki, "The Open Motion Planning Library," *IEEE Robotics & Automation Magazine*, vol. 19, no. 4, pp. 72–82, December 2012, <http://ompl.kavrakilab.org>.
- [21] J. J. Kuffner and S. M. LaValle, "Rrt-connect: An efficient approach to single-query path planning," in *ICRA*, vol. 2, April 2000, pp. 995–1001 vol.2.
- [22] R. Diankov, "Automated construction of robotic manipulation programs," Ph.D. dissertation, Carnegie Mellon University, Robotics Institute, 2010.